A Donor−Acceptor−Donor Bridging Ligand in a Class III Mixed-Valence Complex

Peter J. Mosher,[†] Glenn P. A. Yap,[‡] and Robert J. Crutchley*,[†]

Ottawa-Carleton Chemistry Institute, Carleton University, 1125 Colonel By Drive, Ottawa, Ontario, Canada K1S 5B6, and University of Ottawa, Ottawa, Ontario, Canada K1N 6N5

Received September 26, 2000

The novel mononuclear and dinuclear complexes [Ru(trpy)(bpy)(apc)][PF_6] and [{Ru(trpy)(bpy)}$_2$(μ-adpc)][PF_6]$_2$ (bpy = 2,2′-bipyridine, trpy = 2,2′:6′,2″-terpyridine, apc$^-$ = 4-azo(phenylcyanamido)benzene, and adpc^{2-} = 4,4′-azodi(phenylcyanamido)) were synthesized and characterized by ^{1}H NMR, UV−vis, and cyclic voltammetry. Crystallography showed that the dinuclear Ru(II) complex crystallizes from diethyl ether/acetonitrile solution as [{Ru(trpy)(bpy)}$_2$(μ-adpc)][PF_6]$_2$·2(acetonitrile)·2(diethyl ether). Crystal structure data are as follows: crystal system triclinic, space group $P\bar{1}$, with a, b, and c = 12.480(2), 13.090(3) and 14.147(3) Å, respectively, α, β, and γ = 79.792(3), 68.027(3), and 64.447(3)°, respectively, V = 1933.3(6) Å^3, and Z = 1. The structure was refined to a final R factor of 0.0421. The mixed-valence complex with metal ions, separated by a through-space distance of 19.5 Å, is a class III system, having the comproportionation constant $K_c = 1.3 \times 10^{13}$ and an intervalence band at 1920 nm (ϵ_{max} = 10 000 M^{-1} cm^{-1}), in dimethylformamide solution. The results of this study strongly suggest that the bridging ligand adpc^{2-} can mediate metal−metal coupling through both hole-transfer and electron-transfer superexchange mechanisms.

Introduction

The creation of hybrid polymeric materials that possess useful optical, magnetic, and/or electronic properties requires multidisciplinary research and is a very active field.[1] In this regard, the optoelectronic properties of a polymer depend on the degree of conjugation between units making up the polymer chain. One way of achieving a high degree of extended conjugation, and hence a narrow band gap, has been to synthesize polythiophenes made up of alternating donor/acceptor repeat units.[2] Alternatively, increasing the quinoid character of the polythiophene backbone has been found to have a similar effect.[3] For example, isothianaphthene exhibits a band gap of ca. 1.0 eV, while that of the parent polythiophene is ca. 2.0 eV.[4] At the molecular level, the energy between the highest occupied molecular orbital (HOMO) and the lowest unoccupied molecular orbital (LUMO) is analogous to the macroscopic band gap energy. In addition, the mediation of electronic interactions by a bridging molecule can be quantitatively modeled by the Marcus−Hush theory for mixed-valence systems.[5] Thus, the study of mixed-valence complexes provides the knowledge to purposefully synthesize novel polymeric materials.

The strength of donor−acceptor coupling can range from nonexistent (class I) to weak (class II) to very strong (class III).[6] For a class III complex, there is no thermal barrier for electron transfer between metal ions and, thus, the odd electron exists in a delocalized state. Metal−metal coupling gives rise to a metal-to-metal charge transfer (MMCT) transition in the complex's electronic absorption spectrum, and the stability of a mixed-valence complex [III,II] relative to its oxidized and reduced forms can be quantified by the comproportionation equilibrium constant K_c:

$$[\mathrm{III,III}] + [\mathrm{II,II}] \overset{K_c}{\rightleftharpoons} 2[\mathrm{III,II}] \qquad (1)$$

This permits the calculation of the free energy of comproportionation ($\Delta G_c = -RT \ln(K_c)$), which is made up of the free energy terms[7]

$$\Delta G_c = \Delta G_s + \Delta G_e + \Delta G_i + \Delta G_r + \Delta G_{AF} \qquad (2)$$

where ΔG_s reflects the statistical distribution of the comproportionation equilibrium, ΔG_e accounts for the electrostatic repulsion of the two like-charged metal centers, ΔG_i is an inductive factor dealing with competitive coordination of the bridging ligand by the metal ions, ΔG_r is the free energy of resonance exchange, and ΔG_{AF} is the free energy of antiferromagnetic exchange. When metal−metal coupling is very strong, the resonance exchange term ΔG_r largely determines the magnitude of ΔG_c.[7]

Pentaammineruthenium dinuclear complexes incorporating various bridging ligands have played an important role in understanding how the medium influences coupling in mixed-valence systems.[8,9] For example, [{Ru(NH$_3$)$_5$}$_2$(μ-4,4′-bipyridine)]$^{5+}$ is a class II system having K_c = 20 and an MMCT band centered at 1030 nm (ϵ = 920 M^{-1} cm^{-1}).[10] Its solvent-dependent properties are largely consistent with the predictions of Hush theory.[8] Inserting an azo group between the pyridine groups of the bridging ligand does not appear to dramatically effect coupling. Thus, [{Ru(NH$_3$)$_5$}$_2$(μ-4,4′-azopyridine)]$^{5+}$ is

[†] Carleton University.
[‡] University of Ottawa.

(1) Allcock, H. *Science* **1992**, *255*, 1106.
(2) Zhang, Q. T.; Tour, J. M. *J. Am. Chem. Soc.* **1998**, *120*, 5355.
(3) Kitamura, C.; Tanaka, S.; Yamashita, Y. *Chem. Mater.* **1996**, *8*, 570.
(4) Kobayashi, M.; Colaneri, M.; Boysel, M.; Wudl, F.; Heeger, A. J. *J. Phys. Chem.* **1985**, *82*, 5717.
(5) Brunschwig, B. S.; Sutin, N. *Coord. Chem. Rev.* **1999**, *187*, 233.
(6) Robin, M. B.; Day, P. *Adv. Inorg. Chem. Radiochem.* **1967**, *10*, 247.
(7) Evans, C. E. B.; Naklicki, M. L.; Rezvani, A. R.; White, C. A.; Kondratiev, V. V.; Crutchley, R. J. *J. Am. Chem. Soc.* **1998**, *120*, 13096.
(8) Creutz, C. *Prog. Inorg. Chem.* **1983**, *30*, 1.
(9) Crutchley, R. J. *Adv. Inorg. Chem.* **1994**, *41*, 273.
(10) Sutton, J. E.; Sutton, P. M.; Taube, H. *Inorg. Chem.* **1979**, *18*, 1017.

10.1021/ic001268u CCC: $20.00
Published on Web 02/07/2001

a class II system having $K_c = 40$ and an MMCT band centered at 1400 nm ($\epsilon = 500\ M^{-1}\ cm^{-1}$).[11] However, if a disulfide group is inserted, coupling dramatically increases. [{$Ru(NH_3)_5$}$_2$(μ-4,4′-disulfidebipyridine)]$^{5+}$ is a strongly coupled class II system having $K_c = 8 \times 10^4$ and an MMCT band centered at 1500 nm ($\epsilon = 4300\ M^{-1}\ cm^{-1}$).[12] As pyridine possesses low-energy π^* orbitals that permit it to act as a π-acceptor ligand and disulfide is expected to be a π donor, this suggested to us that alternating donor and acceptor groups in a bridging ligand might lead to strong metal−metal coupling.

In this study, we have applied the above rationale to previous work[13] on the weakly coupled ($K_c = 16$) mixed-valence complex, [{$Ru(NH_3)_5$}$_2$(μ-bp)]$^{3+}$, where bp^{2-} is

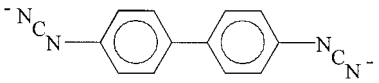

and have synthesized the novel bridging ligand 4,4′-azodi(phenylcyanamide) dianion, adpc^{2-}

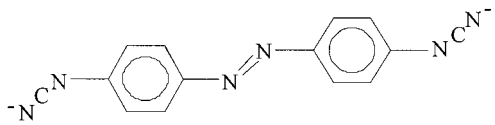

The Ru(II) dinuclear complex [{Ru(trpy)(bpy)}$_2$(μ-adpc)][PF_6]$_2$ (bpy = 2,2′-bipyridine, trpy = 2,2′:6′,2″-terpyridine, and adpc^{2-} = 4,4′-azodi(phenylcyanamido)) was also synthesized and characterized by ^{1}H NMR, UV−vis, cyclic voltammetry, and crystallography. One-electron oxidation of this complex yields a mixed-valence system whose properties are consistent with class III behavior, despite metal ions being separated by 19.5 Å. The nature of the bridging ligand adpc^{2-} was investigated by ab initio methods to understand its effectiveness at mediating metal−metal coupling.

Experimental Section

Equipment. UV−vis spectroscopy was performed on a CARY 5 UV−vis−near-IR spectrophotometer. IR spectra were taken with a BOMEM Michelson-100 FT-IR spectrophotometer (KBr disks). ^{1}H NMR data from dimethyl sulfoxide-d_6 solutions were obtained by using a Bruker AMX-400 spectrometer or a Varian Gemini 200 spectrometer. Cyclic voltammetry was performed using a BAS CV-27 voltammograph and plotted on a BAS XY recorder. The sample cell consisted of a double-walled glass crucible with an inner volume of ~15 mL, which was fitted with a Teflon lid incorporating a three-electrode system and argon bubbler. The cell temperature was maintained at 25.0 ± 0.1 °C by means of a HAAKE D8 recirculating bath. BAS 2013 Pt electrodes (1.6 mm diameter) were used as the working and counter electrodes. A silver wire functioned as a pseudo-reference electrode. Acetonitrile (MeCN) was dried over P_2O_5 and vacuum-distilled. Nitromethane ($MeNO_2$) and dimethylformamide (DMF) were dried with anhydrous alumina and vacuum-distilled. Tetrabutylammonium hexafluorophosphate (TBAH), purchased from Aldrich, was twice recrystallized from 1:1 ethanol/water and vacuum-dried at 110 °C. Ferrocene ($E° = 0.665$ V vs NHE) and cobaltocenium hexafluorophosphate ($E° = -0.664$ V vs NHE) were used as internal references.[14] An OTTLE cell was used to perform the spectroelectrochemistry.[15] The cell had interior dimensions of roughly 1 × 2 cm with a path length of 0.2 mm and was fitted with gold-foil working and counter electrodes and a silver/silver chloride reference electrode. OTTLE work done in DMF used ITO (indium−tin oxide) coated glass for the working and counter electrodes. Elemental analyses were performed by Canadian Microanalytical Services.

Materials. All of the reagents and solvents used were reagent grade or better. 4,4′-Azodianiline was purchased from ACROS Organics and used as received. Synthesis of [Ru(trpy)(bpy)Cl][PF_6] has been previously described.[16] ITO glass plates were purchased from Delta-Technologies.

Preparation of 4,4′-Azodi(phenylcyanamide)·H_2O (adpcH_2). Ammonium thiocyanate (1.5 g, 20 mmol) was dissolved in 20 mL of acetone and brought to a boil. To this was added dropwise a solution of benzoyl chloride (2.8 g, 20 mmol) in 20 mL of acetone, and the mixture was refluxed for an additional 15 min. 4,4′-Azodianiline (2.1 g, 9.9 mmol) was dissolved in 150 mL of boiling acetone and then slowly added to the refluxing mixture above. The mixture was refluxed for 1 h and then poured into a beaker containing 800 mL of water. The brown benzoyl thiourea precipitate was removed by suction filtration and dissolved in 300 mL of boiling 2 M NaOH. The resulting deep red solution was boiled for 5 min and then cooled to 60 °C. Lead acetate (7.5 g, 20 mmol) was dissolved in 20 mL of water and added to the thiourea solution. The temperature was maintained at 60 °C for 15 min, forming a black PbS precipitate, and the mixture was then filtered by suction into an ice-cooled flask. The filtrate was acidified to pH 5 with the addition of 25 g of glacial acetic acid, and a green precipitate was removed by suction filtration. Recrystallization from 700 mL of boiling acetone afforded a greenish gold solid. Yield: 1.3 g, 51%. Anal. Calcd for $C_{14}H_{12}N_6O$: C, 59.99; H, 4.32; N, 29.98. Found: C, 59.70; H, 4.39; N, 29.76. IR: ν(NCN) 2225 cm^{-1}. ^{1}H NMR (400 MHz): 10.63 (2H, broad singlet), 7.89 (4H, doublet), 7.13 (4H, doublet) ppm. Mp: 200−205 °C dec.

Preparation of Tl_2[adpc]. A 0.25 g (0.95 mmol) portion of adpcH_2 was dissolved in 300 mL of boiling 2/1 acetone/water solution. To this was added a 50 mL 2/1 acetone/water solution of thallium acetate (0.53 g, 2.0 mmol). An orange precipitate quickly formed with the addition of 1 mL of triethylamine. The mixture was boiled for 2 min longer and then slowly cooled to −20 °C. Filtration afforded a bright orange microcrystalline solid, which was washed with cold water and acetone. Yield: 0.53 g, 83%. Anal. Calcd for $C_{14}H_8N_6Tl_2$: C, 25.13; H, 1.21; N, 12.56. Found: C, 25.51; H, 1.31; N, 12.57. IR: ν(NCN) 2078 and 2042 cm^{-1}. ^{1}H NMR (200 MHz): 7.41 (4H, doublet), 6.62 (4H, doublet) ppm. Mp: 200−205 °C dec.

The poor solubility of Tl_2[adpc] in DMF limited the accuracy of the cyclic voltammetry study. This was corrected by preparing the tetraphenylarsonium salt.

Preparation of [AsPh]$_2$[adpc]·H_2O. adpcH_2 (0.098 g, 0.37 mmol) was dissolved in 50 mL of 2 M $NaOH_{aq}$. To this was added a solution of [$AsPh_4$]Cl·H_2O (0.35 g, 0.80 mmol) in 20 mL of water, and the mixture was stirred for 15 min. The red precipitate was collected and washed with 30 mL of water and then recrystallized from boiling MeCN. Yield: 0.25 g, 66%. Anal. Calcd for $C_{62}H_{50}N_6OAs_2$: C, 71.26; H, 4.82; N, 8.04. Found: C, 70.91; H, 4.95; N, 8.06. The ^{1}H NMR spectrum of adpc^{2-} is nearly identical with that obtained for Tl_2[adpc]. ^{1}H NMR (200 MHz): 7.78 (40H, multiplet), 7.39 (4H, doublet), 6.59 (4H, doublet) ppm.

Preparation of [{Ru(trpy)(bpy)}$_2$(μ-adpc)][PF_6]$_2$·(ether). [Ru(bpy)(trpy)Cl][PF_6] (0.60 g, 0.89 mmol) was dissolved in 100 mL of DMF in a 250 mL round-bottom flask. Tl_2[adpc] (0.30 g, 0.45 mmol) was added, and the deep red solution was refluxed for 48 h. The reaction mixture was then chilled to −20 °C and filtered to remove a fine white TlCl precipitate. The filtrate was then concentrated to 30 mL by rotary evaporation, and 600 mL of ether was added to precipitate the crude product, which was then collected by suction filtration (0.56 g). The crude product (0.3 g) was dissolved in 60 mL of 1:1 MeCN/toluene, filtered, and purified by chromatography on a 50 cm × 3 cm diameter

(11) Launay, J.-P.; Tourrel-Paagis, M.; Libskier, J.-F.; Marvaud, V.; Joachim, C. *Inorg. Chem.* **1991**, *30*, 1033.
(12) de Sousa Moreira, I.; Franco, D. W. *J. Chem. Soc., Chem. Commun.* **1992**, 450.
(13) Aquino, M. A. S.; White, C. A.; Bensimon, C.; Greedan, J. E.; Crutchley, R. J. *Can. J. Chem.* **1996**, *74*, 2201.
(14) Gennett, T.; Milner, D. F.; Weaver, M. J. *J. Phys. Chem.* **1985**, *89*, 2787.
(15) (a) Krejcik, M.; Danek, M.; Hartl, F. *J. Electroanal. Chem. Interfacial Electrochem.* **1991**, *317*, 179. (b) Evans, C. E. B. Ph.D. Thesis, Carleton University, 1997.
(16) Takeuchi, K. J.; Thompson, M. S.; Pipes, D. W.; Meyer, T. J. *Inorg. Chem.* **1984**, *23*, 1845.

column containing ~250 g grade III alumina (Brockmann I, weakly acidic, 150 mesh). Three bands containing starting material and a mononuclear complex were eluted with 1:1 MeCN/toluene. A fourth band was eluted with 500 mL of 3:1 MeCN/toluene and contained the target complex, which crystallized from the solution upon evaporation of the MeCN. Recrystallization was achieved by the slow diffusion of ether into a saturated solution of the complex in MeCN. Yield: 0.16 g (43%). Anal. Calcd for $C_{68}H_{56}N_{16}OP_2F_{12}Ru_2$: C, 50.88; H, 3.52; N, 13.96. Found: C, 50.81; H, 3.33; N, 14.04. IR: ν(NCN) 2161 cm^{-1}. ^{1}H NMR (400 MHz): 9.65 (2H, doublet), 8.96 (2H, doublet), 8.90 (4H, doublet), 8.78 (4H, doublet), 8.69 (2H, doublet), 8.40 (2H, triplet), 8.32 (2H, triplet), 8.09 (6H, multiplet), 7.85 (2H, triplet), 7.73 (4H, doublet), 7.46 (6H, multiplet), 7.27 (4H, doublet), 7.15 (2H, triplet), 6.02 (4H, doublet) ppm.

Preparation of 4-Azo(phenylcyanamide)benzene Hydrate (apcH). The same procedure as that for adpcH_2 was followed. Recrystallization from acetone/water (3/1) gave orange needles and crystalline flakes of the product. Yield: 60%. Anal. Calcd for $C_{13}H_{11}N_4O_{0.5}$: C, 67.52; H, 4.79; N, 24.23. Found: C, 67.55; H, 4.79; N, 24.66. IR: ν(NCN) 2222 cm^{-1}. ^{1}H NMR (400 MHz): 10.71 (1H, broad singlet), 7.95 (2H, doublet), 7.87 (2H, doublet), 7.58 (3H, multiplet), 7.17 (2H, doublet) ppm. Mp: 154−157 °C.

Preparation of Tl[apc]. A procedure identical with that employed to synthesize Tl_2[adpc] was used. Orange crystalline flakes were isolated directly from the reaction solution. Yield: 73%. Anal. Calcd for $C_{13}H_9N_4Tl$: C, 36.69; H, 2.13; N, 13.16. Found: C, 36.53; H, 2.14; N, 13.29. IR: ν(NCN) 2075 and 2042 cm^{-1}.

Preparation of [Ru(trpy)(bpy)(apc)][PF$_6$]. The mononuclear complex was synthesized in the same manner as the dinuclear species above, except that only a 1/1 ratio of [Ru(trpy)(bpy)Cl]$^+$ and ligand was used. Yield: 53%. Anal. Calcd for $C_{38}H_{28}N_9F_6PRu$: C, 53.27; H, 3.29; N, 14.71. Found: C, 53.48; H, 3.42; N, 14.41. IR: ν(NCN) 2161 cm^{-1}. ^{1}H NMR (400 MHz): 9.65 (1H, doublet), 8.95 (1H, doublet), 8.91 (2H, doublet), 8.79 (2H, doublet), 8.69 (1H, doublet), 8.40 (1H, triplet), 8.34 (1H, triplet), 8.10 (3H, multiplet), 7.86 (1H, triplet), 7.72 (4H, multiplet), 7.46 (8H, multiplet), 7.15 (1H, triplet), 6.08 (2H, doublet) ppm.

Crystallography. Plates of [{Ru(trpy)(bpy)}$_2$(μ-adpc)][PF$_6$]$_2$·2(acetonitrile)·2(diethyl ether) were grown by slow diffusion of diethyl ether into an acetonitrile solution of the complex. The data were collected on a 1K Siemens Smart CCD using Mo Kα radiation (λ = 0.710 73 Å) at 203(2) K using an ω-scan technique and corrected for absorptions using equivalent reflections.[17] No symmetry higher than triclinic was observed, and solution in the centric space group option yielded chemically reasonable and computationally stable results of refinement. The structure was solved by direct methods and refined with full-matrix least-squares procedures. The molecular cation is located at an inversion center. A molecule of acetonitrile and a molecule of diethyl ether are each located cocrystallized in the asymmetric unit. Anisotropic refinement was performed on all non-hydrogen atoms. All hydrogen atoms were calculated. Scattering factors are contained in the SHELXTL 5.1 program library.

Results

The complexes of this study were synthesized by the metathesis reaction of [Ru(trpy)(bpy)Cl]$^+$ with the thallium salts of apc$^-$ or adpc^{2-} in refluxing DMF. Some purification by column chromatography was required, but the complexes were nevertheless isolated in good yields. We observed no evidence for a photoinduced *cis*−*trans* isomerization of the azo group,[18] but these studies were preliminary, and it may be that isomerization back to the more stable trans isomer is rapid.[19] Both Ru(II) complexes are air-stable and can be readily recrystallized. We also attempted to prepare the analogous pentaammineruthenium(III) dinuclear complex but were unsuccessful in obtaining a product that gave a reasonable elemental analysis.

Table 1. Crystal Data for [{Ru(trpy)(bpy)}$_2$(μ-adpc)][PF$_6$]$_2$·2(acetonitrile)·2(diethyl ether)

formula	$C_{76}H_{72}F_{12}N_{18}O_2P_2Ru_2$
fw	1761.60
cryst syst	triclinic
space group	$P\bar{1}$
unit cell dimens	
a, *b*, *c*/Å	12.480(2), 13.090(3), 14.147(3)
α, β, γ/deg	79.792(3), 68.027(3), 64.477(3)
V/Å^3	1933.3(6)
Z	1
calcd density/(g/cm^3)	1.513
cryst dimens/mm	0.30 × 0.15 × 0.04
θ range/deg	1.72−28.83
limiting indices	$-15 \le h \le 16$, $-17 \le k \le 17$, $0 \le l \le 18$
no. of rflns collected	15 188
no. of unique rflns	8763
abs cor	semiempirical from equivalents
transmissn range	0.928 078−0.690 280
R1, wR2 ($I > 2\sigma(I)$)[a]	R1 = 0.0421, wR2 = 0.0682
goodness-of-fit on F^2	1.044

[a] $R1 = \sum||F_o| - |F_c||/\sum|F_o|$; $wR2 = (\sum w(|F_o| - |F_c|)^2/\sum w|F_o|^2)^{1/2}$.

Table 2. Selected Crystal Structure Data for [{Ru(trpy)(bpy)}$_2$(μ-adpc)][PF$_6$]$_2$·2(acetonitrile)·2(diethyl ether)

Bond Lengths[a]/Å			
Ru−N(1)	2.041(2)	N(6)−C(26)	1.164(3)
Ru−N(2)	2.069(2)	N(7)−C(26)	1.281(4)
Ru−N(3)	2.065(2)	N(7)−C(27)	1.394(3)
Ru−N(4)	1.964(2)	N(8)−C(30)	1.420(3)
Ru−N(5)	2.062(2)	N(8)−N(8A)	1.274(4)
Ru−N(6)	2.046(2)		
Bond Angles[a]/deg			
N(1)−Ru−N(2)	78.98(9)	N(4)−Ru−N(5)	79.50(10)
N(1)−Ru−N(5)	91.37(9)	N(6)−C(26)−N(7)	173.1(3)
N(3)−Ru−N(2)	99.81(9)	C(26)−N(6)−Ru	164.4(2)
N(4)−Ru−N(3)	79.75(9)	C(26)−N(7)−C(27)	118.7(2)
N(5)−Ru−N(2)	100.94(9)	N(8A)−N(8)−C(30)	114.0(3)

[a] Estimated standard deviations are in parentheses.

Deep red-brown plates of the dinuclear Ru(II) complex [{Ru(trpy)(bpy)}$_2$(μ-adpc)]$^{2+}$ that were suitable for crystallography were grown by diffusion of ether into a solution of the complex in acetonitrile. Crystallography data and bond lengths and angles are reported in Tables 1 and 2, respectively. An ORTEP drawing of the complex cation is shown in Figure 1. The Ru(II) ion occupies a pseudo-octahedral coordination sphere of nitrogen donor atoms where the cyanamide group of the phenylcyanamide ligand is trans to a pyridine moiety of the bipyridine ligand. The bridging adpc^{2-} ligand is approximately planar, with the cyanamide groups in an *anti* conformation relative to each other and the azo group adopting the more thermodynamically stable trans conformation. The planar geometry of the adpc^{2-} bridging ligand is suggested to allow for a more effective π delocalization of the cyanamide groups with phenyl and azo groups. This rationale has also been used to explain the planar conformation of the 1,4-dicyanamidobenzene dianion and its derivatives, observed in crystal structures of tetraphenylarsonium salts[20] and Ru(III) complexes.[21] The cyanamide group is approximately

(17) Blessing, R. *Acta Crystallogr*. **1995**, *A51*, 33.
(18) Yutaka, T.; Kurihara, M.; Kubo, K.; Nishihara, H. *Inorg. Chem.* **2000**, *39*, 3438.
(19) Chambers, E. J.; Haworth, I. S. *J. Chem. Soc., Chem. Commun.* **1994**, 1631.
(20) Aquino, M. A. S.; Crutchley, R. J.; Lee, F. L.; Gabe, E. J.; Bensimon, C. *Acta Crystallogr*. **1993**, *C49*, 1543.
(21) (a) Aquino, M. A. S.; Lee, F. L.; Gabe, E. J.; Bensimon, C.; Greedan, J. E.; Crutchley, R. J. *J. Am. Chem. Soc*. **1992**, *114*, 5130. (b) Rezvani, A. R.; Bensimon, C.; Cromp, B.; Reber, C.; Greedan, J. E.; Kondratiev, V.; Crutchley, R. J. *Inorg. Chem*. **1997**, *36*, 3322. (c) Evans, C. E. B.; Yap, G. P. A.; Crutchley, R. J. *Inorg. Chem*. **1998**, *37*, 6161.

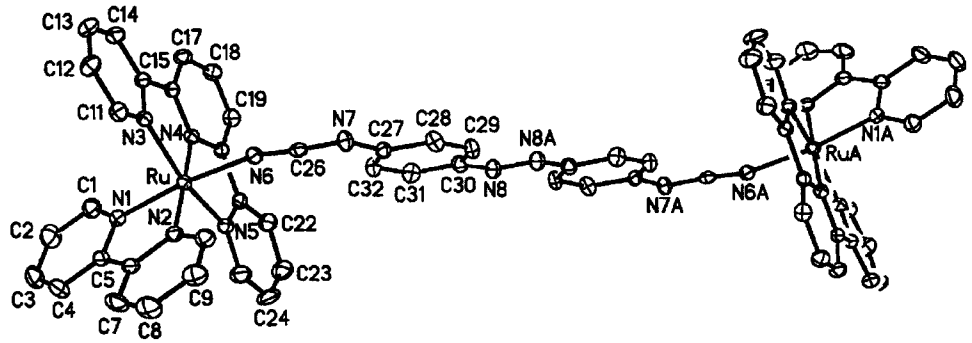

Figure 1. ORTEP drawing of $[\{Ru(trpy)(bpy)\}_2(\mu\text{-adpc})]^{2+}$. The counterions, hydrogen atoms, and solvents of crystallization (two acetonitrile, two diethyl ether) have been omitted for clarity.

Table 3. Cyclic Voltammetry Data[a] of Azo Ligands and Ru(trpy)(bpy) Complexes

ligand/complex	Ru(III/II)	L(1−/2−)	L(0/1−)
Tl[apc]			0.86[b,d]
$[AsPh_4]_2$[adpc]		0.48[b]	0.63[b,e]
$[\{Ru(trpy)(bpy)(apc)\}]^+$	0.96[c]		
	1.06[b]		
$[\{Ru(trpy)(bpy)\}_2(\mu\text{-adpc})]^{2+}$	0.79,[c] 1.57[c]		
	0.91,[b] ∼1.6[b]		
$[\{Ru(trpy)(bpy)(2,4\text{-}Cl_2pcyd)\}]^+$ [f]	1.0[b]		
$[\{Ru(trpy)(bpy)\}_2(\mu\text{-dicyd})]^{2+}$ [g]	0.69,[b] 0.25[b]		

[a] Conditions: in V vs NHE at 25 °C; scan rate of 0.1 V/s; 0.1 M TBAH electrolyte; ferrocene ($Fc^+/Fc = 0.665$ V vs NHE) or cobaltocenium hexafluorophosphate ($E° = -0.664$ V vs NHE) used as internal references. [b] In DMF. [c] In MeCN. [d] Anodic wave only. [e] Partially reversible. [f] Data from ref 25. [g] Data from ref 26.

linear (173.1(3)°), as expected, while the angle describing the coordination of its terminal nitrogen to Ru(II) (164.4(2)°) is significantly bent. In contrast, four crystal structures of Ru(III)−cyanamide complexes showed an average Ru(III)−cyanamide bond angle of 174.6°.[21,22] We have suggested[23] that the π bonding between Ru(III) and cyanamide is optimized when this angle is linear, a condition which evidently relaxed when π bonding is not as important.

Cyclic voltammetry data for the thallium salt of apc^-, the tetraphenylarsonium salt of $adpc^{2-}$, and the two complexes have been placed in Table 3, and a figure showing the cyclic voltammograms of the complexes has been placed in the Supporting Information. The Ru(III/II) couple of $[Ru(trpy)(bpy)(apc)]^+$ in acetonitrile is partially reversible and occurs at a potential of 0.96 V vs NHE. Scanning to more positive potentials resulted in decomposition of the complex and loss of the cathodic wave for the Ru(III/II) couple. The voltammogram of the dinuclear complex $[\{Ru(trpy)(bpy)\}_2(\mu\text{-adpc})]^{2+}$ in acetonitrile shows two Ru(III/II) oxidation waves at 1.57 and 0.79 V vs NHE. The Ru(III/II) couples were quasi-reversible, with the separation between cathodic and anodic waves dependent upon the scan rate. On the basis of the difference between Ru(III/II) couples, the comproportionation equilibrium constant for $[\{Ru(trpy)(bpy)\}_2(\mu\text{-adpc})]^{3+}$ is very large at $K_c = 1.3 \times 10^{13}$ and implies strong metal−metal coupling in the mixed-valence complex.

The bpy and trpy ligand reductions in similar complexes occur between −1 and −2 V vs NHE, with the first reduction wave, assigned[24] to trpy (0/−1), showing some reversibility. In the case of the dinuclear complex, reduction of the azo group of the bridging ligand at these potentials appears to result in loss of reversibility, as there is evidence of electrode deposition (a cathodic spike appeared at −1.44 V vs NHE). This chemistry was not pursued.

In Table 3, we have placed the Ru(III/II) couples[25,26] of $[Ru(trpy)(bpy)(2,4\text{-}Cl_2pcyd)]^+$ and $[\{Ru(trpy)(bpy)\}_2(\mu\text{-dicyd})]^{2+}$ for comparison with the analogous complexes of apc^- and $adpc^{2-}$ ligands. The Ru(III/II) couple of a mononuclear ruthenium complex approximates the energy of a ruthenium ion that is not stabilized by the resonance exchange experienced by ruthenium ions in a dinuclear mixed-valence complex, provided their coordination spheres are similar. Qualitatively, it is expected that, for a dinuclear complex, the Ru(III/II) couple forming the [III,II] complex should be more positive of this value, while the Ru(III/II) couple forming the [II,II] complex should be more negative of this value. Thus, in Table 3, the Ru(III/II) couples of the apc^- and $adpc^{2-}$ complexes approximately follow the expected behavior, but the phenylcyanamide and $dicyd^{2-}$ complexes do not. The reason for this is that antiferromagnetic exchange in $[\{Ru(trpy)(bpy)\}_2(\mu\text{-dicyd})]^{4+}$ stabilizes the [III,III] complex relative to the mixed-valence complex, thereby shifting the corresponding Ru(III,II) couple to more negative potential.[27] This implies that antiferromagnetic exchange is not important in $[\{Ru(trpy)(bpy)\}_2(\mu\text{-adpc})]^{4+}$. Unfortunately, the instability of this [III,III] complex prevented solid-state magnetic measurements.

The electronic absorption data of the thallium(I) salts of apc^- and $adpc^{2-}$ and their Ru(II) and Ru(III) complexes in DMF have been placed in Table 4. The anionic ligands in DMF show a strong visible absorption, which we have assigned to a cyanamide-to-azo group intraligand charge transfer (ILCT) transition. When these ligands are incorporated into the Ru(II) complex, this transition is still observed, but it is now approximately coincident in energy with metal-to-ligand charge transfer (MLCT) transitions of the Ru(II)−bpy and Ru(II)−trpy chromophores.

Spectroelectrochemical studies of the thallium salt of $adpc^{2-}$ in DMF solution are shown in Figure 2. Upon one-electron oxidation of $adpc^{2-}$, the intense absorption of the intraligand

(22) Crutchley, R. J.; McCaw, K.; Lee, F. L.; Gabe, E. J. *Inorg. Chem.* **1990**, *29*, 2576.
(23) Zhang, W.; Bensimon, C.; Crutchley, R. J. *Inorg. Chem.* **1993**, *32*, 5808.
(24) (a) Calvert, J. M.; Schmehl, R. H.; Meyer, T. J. *Inorg. Chem.* **1983**, *22*, 2151. (b) Berger, R. M.; McMillin, D. R. *Inorg. Chem.* **1988**, *27*, 4245.
(25) Mosher, P.; Yap, G. P. A.; Crutchley, R. J. *Inorg. Chem.*, in press.
(26) Rezvani, A. R.; Evans, C. E. B.; Crutchley, R. J. *Inorg. Chem.* **1995**, *34*, 4600.
(27) Antiferromagnetic exchange constants have been measured for $[\{(NH_3)_5Ru\}_2(\mu\text{-L})]^{4+}$, where L is a 1,4-dicyanamidobenzene derivative, and so antiferromagnetic exchange seems certain to make a considerable contribution in $[\{Ru(trpy)(bpy)\}_2(\mu\text{-dicyd})]^{4+}$. See refs 21a and: Naklicki, M. L.; White, C. A.; Plante, L. L.; Evans, C. E. B.; Crutchley, R. J. *Inorg. Chem.* **1998**, *37*, 1880.

Table 4. Electonic Spectral Data[a] for apc$^-$ and adpc^{2-} and Their Ru(II) and Ru(III) Complexes and the Radical Anion adpc$^{\bullet-}$

compd	absorption
[apc][c]	325[b] (4500), 490 (40 300)
[adpc]$^{2-}$	340 (6700), 500 (54 400), 523 (51 500)
[adpc]$^-$	421 (18 400), 498 (31 100), 658 (5030), 714 (17 400), 1310 (3900)
[Ru(trpy)(bpy)(apc)]$^+$	293 (43 200), 318 (38 000), 469 (35 000)
[Ru(trpy)(bpy)(apc)]$^{2+}$	289 (45 300), 311 (41 600), 448 (10 600), 1179 (3960)
[{Ru(trpy)(bpy)}$_2$(μ-adpc)]$^{2+}$	293 (81 900), 317 (72 100), 490 (69 100)
[{Ru(trpy)(bpy)}$_2$(μ-adpc)]$^{3+}$	292 (86 900), 314 (76 700), 471 (41 300), 652 (13 900), 812 (12 700), 1920 (10 000)
[{Ru(trpy)(bpy)}$_2$(μ-adpc)]$^{4+}$	312 (73 400), 456 (41 900), 856 (12 000)

[a] Conditions: in nm; molar extinction coefficient (L mol^{-1} cm^{-1}) appears in parentheses; in 0.1 M TBAH in DMF. [b] Shoulder. [c] DMF solution.

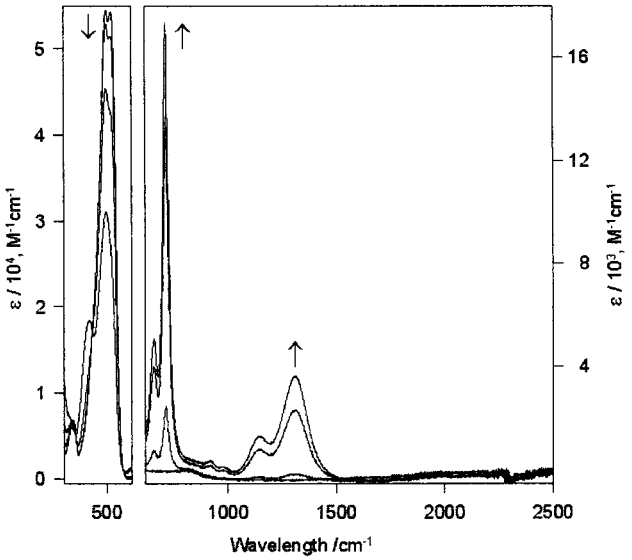

Figure 2. OTTLE cell vis−near-IR spectra showing the oxidation of adpc^{2-} to the radical anion adpc$^-$, in 0.1 M TBAH in DMF, at 25 °C.

charge-transfer band centered at 498 nm loses intensity and two new bands of weaker intensity appear at 714 and 1310 nm that we assign to $\pi \rightarrow \pi$ transitions of the radial anion adpc$^-$. The spectral changes that are seen in Figure 2 are reversible if reduction is performed rapidly. However, further oxidation to adpc^0 is irreversible, as even partial regeneration of the adpc^{2-} spectrum was not achieved.

The spectroelectrochemistry of the [II,II] complex in DMF to generate [III,II] and [III,III] spectra is shown in Figure 3 while the spectra resulting from the stepwise oxidation of [Ru(trpy)(bpy)(apc)]$^+$ have been placed in the Supporting Information. For [Ru(trpy)(bpy)(apc)]$^+$, oxidation of Ru(II) is expected to result in the loss of the MLCT transition in the visible and the appearance of two new absorption bands due to the Ru(III)−cyanamide LMCT chromophore.[28] Only the band at 1179 nm in the spectrum of [Ru(trpy)(bpy)(apc)]$^{2+}$ (Table 4 and Supporting Information) can be unambiguously assigned to this

(28) (a) Crutchley, R. J.; Naklicki, M. L. *Inorg. Chem.* **1989**, *28*, 1955. (b) Evans, C. E. B.; Ducharme, D.; Naklicki, M. L.; Crutchley, R. J. *Inorg. Chem.* **1995**, *34*, 1350.

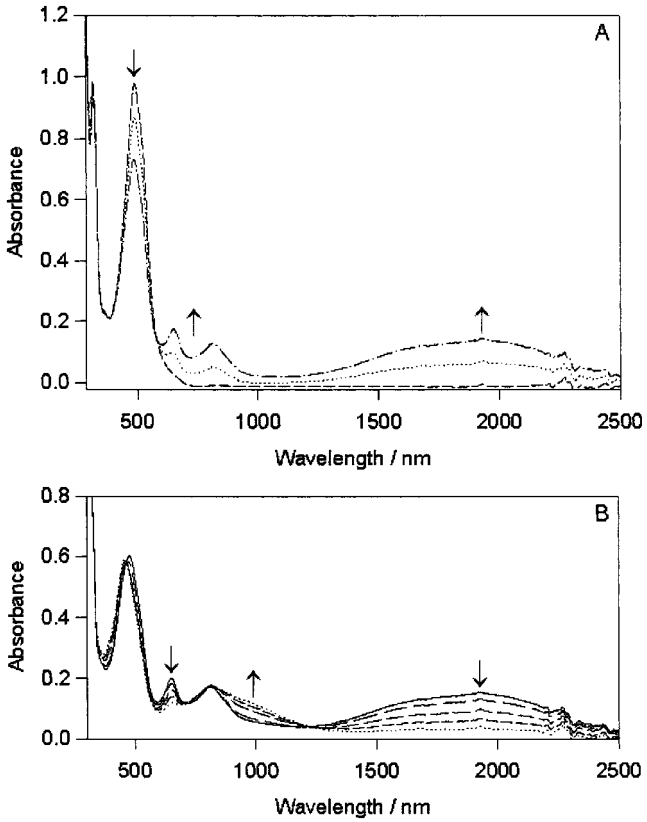

Figure 3. OTTLE cell vis−near-IR spectra of [{Ru(trpy)(bpy)}$_2$(μ-adpc)]$^{2+}$ under increasing anodic potential in 0.1 M TBAH in DMF at 25 °C: (A) 0−0.75 V; (B) 0.80−1.05 V (versus Ag|AgCl).

LMCT chromophore, as the band at 448 nm is derived from ILCT and possibly LMCT transitions.

For [{Ru(trpy)(bpy)}$_2$(μ-adpc)]$^{2+}$, oxidation to the mixed-valence complex results in the appearance of three new spectral features at λ_{max} 652, 812, and 1920 nm (Figure 3A). The band at 812 nm is assigned to the Ru(III)−cyanamide chromophore, as it appears to gain absorptivity with the formation of the [III,III] complex (Figure 3B). However, the band at 652 nm decreases in intensity with the formation of [III,III] (Figure 3B). We tentatively assign this band to a Ru(II)−adpc MLCT transition, as ab initio studies of adpc^{2-} (see Discussion) do show a low-energy LUMO of π symmetry. The intense absorption centered at 1920 nm (Figure 3A) is absent in the spectrum of [II,II] and [III,III] complexes (parts A and B of Figure 3) and is not present in the spectrum of adpc$^-$ (Figure 2). As the appearance of this band is most likely associated with the oxidation of Ru(II), we have assigned this band to a metal-to-metal charge-transfer MMCT transition.[29] When the

(29) This assignment depends on whether Ru(II) or adpc^{2-} is oxidized in the study shown in Figure 3A. We note that the energies, intensities, and widths of the bands seen for the radical anion adpc$^-$ (Figure 2) are not observed in the spectrum of the mixed-valence complex (Figure 3A). Second, in DMF solution, the potential of the first oxidation couple of the dinuclear complex at 0.91 V vs NHE is close to that of the mononuclear complex at 1.06 V vs NHE (Table 3) and of the Ru(III/II) couples of [Ru(trpy)(bpy)L]$^+$, where L is a phenylcyanamide derivative.[25] It is therefore reasonable to assign the couple at 0.91 V to a Ru(III/II) couple. Finally, we have shown in studies of another redox-active ligand that the redox potentials of the 1,4-dicyanamidebenzene dianion shift to positive potentials by more than 1 V when coordinated to pentaammineruthenium(III). This positive shift is even greater when the ammines are replaced by pyridine moieties.[26] We expect a similar shift in ligand redox potentials when adpc^{2-} is coordinated to terpyridine(bipyridine)ruthenium(III), and this would take the ligand couples outside the potential range that was studied.

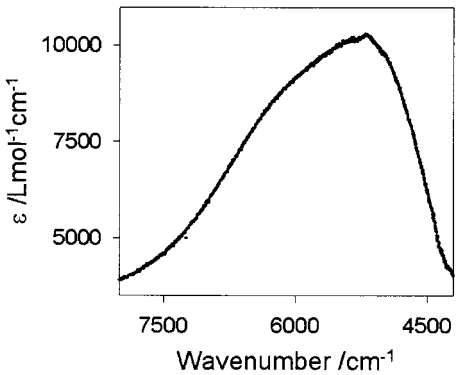

Figure 4. Metal−metal charge-transfer band of $[\{Ru(trpy)(bpy)\}_2(\mu\text{-adpc})]^{3+}$ in 0.1 M TBAH in DMF.

Table 5. Electrochemical and MMCT Band Spectral Data for $[\{Ru(trpy)(bpy)\}_2(\mu\text{-adpc})]^{3+}$ in Various Solvents

	solvent		
	acetonitrile	DMF	nitromethane
λ_{max}[a]/nm	1800 (6900) [0.0935]	1920 (10 000) [0.167]	1830 (8400) [0.119]
$\Delta\nu/cm^{-1}$	2710	2870	2640
$H_{MM'}$[b]/cm^{-1}	2780	2600	2730
ΔE[c]/V	0.775	∼0.7	∼0.8
K_c	1.3×10^{13}	$10^{12}-10^{13}$	$10^{13}-10^{14}$

[a] Wavelength of maximum absorbance (in nm) with the extinction coefficient (M^{-1} cm^{-1}) in parentheses. The oscillator strength is shown in brackets. [b] $H_{MM'} = E_{MMCT}/2$. [c] The oxidation limits of DMF and nitromethane made precise determinations of the second Ru(III/II) oxidation couples difficult.

MMCT band is plotted against an energy axis (Figure 4), the band shape is non-Gaussian with a pronounced high-energy tail, a characteristic of MMCT band properties of a class III complex.[30] This result together with the very large comproportionation constant observed for $[\{Ru(trpy)(bpy)\}_2(\mu\text{-adpc})]^{3+}$ designates this complex as a class III system despite metal ions that are separated by 19.5 Å.[31] We note as well that for a class III complex, the metal−metal coupling element H_{MM} is given by the MMCT band energy band energy:[8,9]

$$H_{MM'} = \frac{E_{MMCT}}{2} \qquad (3)$$

Thus, for $[\{Ru(trpy)(bpy)\}_2(\mu\text{-adpc})]^{3+}$ in DMF, $H_{MM'} = 2600$ cm^{-1}. This is considerably smaller than what might have been predicted on the basis of the magnitude of the comproportionation constant but is not unprecedented in the literature.[32]

Class III complex properties should also be solvent-independent, and so we examined the MMCT properties of $[\{Ru(trpy)(bpy)\}_2(\mu\text{-adpc})]^{3+}$ in nitromethane and acetonitrile as well as DMF (Table 5). Both the energy and bandwidth of the MMCT band change very little with solvent. However, the oscillator strength is significantly greater in DMF compared to that in either acetonitrile or nitromethane.

The [III,III] spectrum in Figure 3B shows the growth of the LMCT bands, as there are now two Ru(III)−cyanamide chromophores per complex. Unfortunately, the [III,III] complex is unstable, as only 90% of the [II,II] spectrum was recovered by reducing [III,III]. The temperature of this experiment was reduced to 0 °C, but no improvement in reversibility was observed. The reversibility from the [III,III] complex in nitromethane or acetonitrile was noticeably poorer.

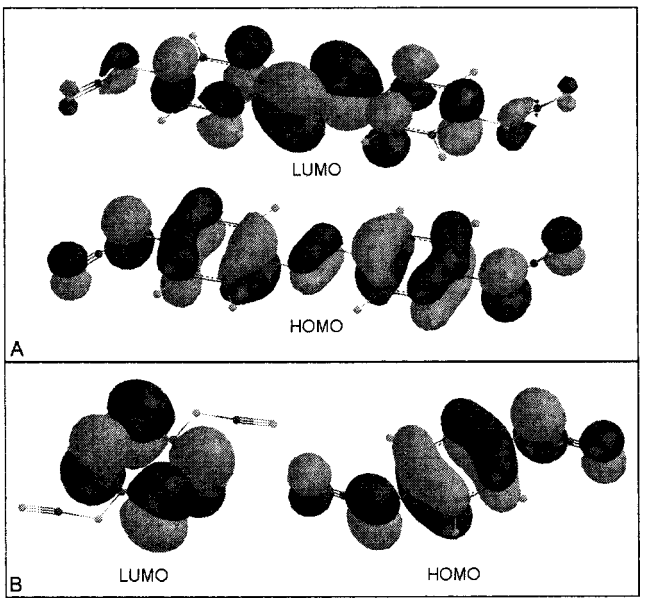

Figure 5. Calculated geometries for the highest occupied molecular orbital (HOMO) and lowest unoccupied molecular orbital (LUMO) of $adpc^{2-}$ (A) and $dicyd^{2-}$ (B).[35]

Discussion

The observation of class III properties in $[\{Ru(trpy)(bpy)\}_2(\mu\text{-adpc})]^{3+}$, despite a metal−metal ion through-space distance of 19.5 Å, is extraordinary. The only comparable class III complex is $[\{Ru(NH_3)_5\}_2(\mu\text{-1,4-benzoquinonediimine})]^{5+}$, in which the ruthenium ions are separated by 10 Å.[33] Indeed, the magnitude of the comproportionation equilibrium constant of $[\{Ru(trpy)(bpy)\}_2(\mu\text{-adpc})]^{3+}$ ($K_c = 1.3 \times 10^{13}$) is second only to that of $[\{Ru(NH_3)_4\}_2(\mu\text{-bptz})]^{5+}$, where bptz is 3,6-bis(2-pyridyl)tetrazine, with $K_c = 10^{15}$ but at a metal−metal separation of 6.8 Å.[34] Why then is $adpc^{2-}$ so effective at mediating metal−metal coupling?

When metal ion separation precludes direct metal−metal orbital overlap, coupling between metal ions necessarily involves bridging ligand orbitals and is therefore defined by superexchange processes. A complete description of superexchange should include the sum of all possible contributions involving the bridging ligand's orbitals. However, it is usually possible to simplify the description to a dominant pathway for superexchange, which in the case of a π-acceptor bridging ligand (e.g., pyridine, pyrazine, etc.) is electron transfer through the lowest unoccupied molecular orbital (LUMO),[8] while for a π-donating ligand (e.g., 1,4-dicyanamidobenzene dianion), it is hole transfer through the highest occupied molecular orbital (HOMO).[7] Because of the cyanamide anion groups, the $adpc^{2-}$ bridging ligand is a π-donor system and might be expected to mediate metal−metal coupling by using the hole transfer mechanism, as does the $dicyd^{2-}$ bridging ligand, but there are important differences.

The results of an ab initio calculation[35] of the HOMO and LUMO of $adpc^{2-}$ and $dicyd^{2-}$ are shown in Figure 5. There

(30) Nelsen, S. F. *Chem. Eur. J.* **2000**, *6*, 581.
(31) Obtained from the Ru(II) dinuclear crystal structure.
(32) See Table 15 of ref 8.
(33) Joss, S.; Reust, H.; Ludi, A. *J. Am. Chem. Soc.* **1981**, *103*, 981.
(34) (a) Johnson, J. E. B.; de Groff, C.; Ruminski, R. R. *Inorg. Chim. Acta* **1991**, *187*, 73. (b) Poppe, J.; Moscherosch, M.; Kaim, W. *Inorg. Chem.* **1993**, *32*, 2640.
(35) Spartan version 5.0.1 calculation using the Hartree−Fock model with the 6-31G** basis set and geometry optimization.

are two important comparisons to make. For dicyd^{2-}, the HOMO−LUMO energy gap is large at 2.59 eV and it is clear that only the HOMO can interact simultaneously with ruthenium donor and acceptor dπ orbitals. For adpc^{2-}, both the HOMO and LUMO have the correct symmetry to interact simultaneously with ruthenium dπ orbitals and the HOMO−LUMO energy gap is only 1.07 eV. Thus, superexchange via both the HOMO and LUMO may be energetically favorable.

The general equation[36] for superexchange coupling of the metal centers

$$H_{MM'} = \frac{H_{ML}H_{M'L}}{2\Delta E_{ML}} + \frac{H_{LM}H_{LM'}}{\Delta E_{LM}} \quad (4)$$

is illustrative of the various factors controlling the metal−metal coupling element $H_{MM'}$. The coupling elements in the two terms on the right of eq 4 are associated with metal−ligand interactions of the electron-transfer and hole-transfer pathways, respectively. The denominators are reduced energy gaps between metal and ligand orbitals. The subscript nomenclature may be understood given that the electron-transfer pathway is associated with metal-to-ligand charge transfer (MLCT) bands in the electronic spectrum of the complex, while the hole-transfer pathway is associated with ligand-to-metal (LMCT) bands.

In the present case, the reduced energy gaps can be readily calculated from charge-transfer data. However, metal−ligand coupling elements will greatly depend on the value chosen for the transition dipole moment length. The largest value it may have is 9.75 Å, which is the halfway point between the two metal ions bridged by adpc^{2-}. Depending upon the degree of covalency in the metal−ligand interaction, the transition dipole moment will be smaller and so a calculation of H_{MM} may not be useful at this time. Nevertheless, the reduced energy gap of the hole-transfer pathway ($\Delta E_{LM} = 9000$ cm^{-1}) is smaller than that of the electron-transfer pathway ($\Delta E_{LM} = 12\,200$ cm^{-1}), and so it seems likely that hole-transfer superexchange makes the greatest contribution to metal−metal coupling in [{Ru(trpy)(bpy)}$_2$(μ-adpc)]$^{3+}$.

Conclusion

We have shown that by alternating donor and acceptor groups within a bridging ligand it is possible to dramatically enhanced metal−metal coupling within a mixed-valence complex. The alternation of donor and acceptor groups reduces the energy gap between the π HOMO and LUMO of adpc^{2-} and, as these orbitals can interact simultaneously with ruthenium ion dπ donor and acceptor orbitals, superexchange via both hole and electron-transfer mechanisms is possible. The magnitude of coupling seen for [{Ru(trpy)(bpy)}$_2$(μ-adpc)]$^{3+}$ ($H_{MM'} = 2600$ cm^{-1} and $K_c = 1.3 \times 10^{13}$), despite a separation of 19.5 Å between ruthenium ions, suggests that the properties of the adpc^{2-} bridging ligand approach that of a truly conducting molecular wire.

Acknowledgment. We are grateful to the Natural Sciences and Engineering Research Council of Canada (NSERC) for financial support.

Supporting Information Available: Figures showing the cyclic voltammograms of [{Ru(trpy)(bpy)}$_2$(μ-adpc)]$^{2+}$.and [Ru(trpy)(bpy)(apc)]$^+$ in acetonitrile and absorption spectra of the spectroelectrochemical oxidation of [Ru(trpy)(bpy)(apc)]$^+$ in DMF and full listings of crystal structure data, atomic parameters, anisotropic thermal parameters, bond lengths, and bond angles, as well as electronic files in CIF format, for [{Ru(trpy)(bpy)}$_2$(μ-adpc)]$^{2+}$. This material is available free of charge via the Internet at http://pubs.acs.org.

IC001268U

(36) Creutz, C.; Newton, M. D.; Sutin, N. *J. Photochem. Photobiol. A: Chem.* **1994**, *82*, 47.